Iran J Sci Technol Trans Sci (2021) 45:753–759
https://doi.org/10.1007/s40995-020-01034-8

RESEARCH PAPER

Determination of Radioactivity in Building Materials and Associated Radiation Hazards by Full Spectrum Analysis Approach

Hossein Bazrafshan[1] · Rahim Khabaz[1]

Received: 3 July 2020 / Accepted: 11 November 2020 / Published online: 5 January 2021

Abstract

In this study, we used the combination of gamma ray spectroscopy and full spectrum analysis method to calculate the radioactivity concentrations of ^{40}K, ^{232}Th and ^{226}Ra radioisotopes in the building materials. The activities of ^{40}K, ^{232}Th and ^{226}Ra were between (36.79 and 559.82), (1.29 and 36.01) and (1.20 and 32.62) Bq kg^{-1}, respectively. The absorbed dose rate in air (D), the annual effective dose rate (AEDR), the radium equivalent activity (Ra_{eq}), the external and internal hazard indices (H_{ex}, H_{in}) in all samples were estimated to assess the level of safety for people living in buildings made of these materials. Finally, the results were compared with international recommended values which showed that applying these materials for construction is not a threat to the population.

Keywords Gamma ray spectrometry · Full-spectrum analysis · Environmental radioactivity · Dose rate · Building materials

1 Introduction

Natural radiation sources are a significant contributor to human and living beings (Arjomandi et al. 2018). Natural radiation is usually classified as either cosmic or terrestrial radiation (Pangh et al. 2019). The main natural contributors to external exposure from gamma radiation are uranium and thorium series together with potassium (El-Taher et al. 2007). The radioactivity of building materials is not the same in different parts of the world and may vary from one place to another in one area, depending on the geological structure of that region (Khabaz and Hassanvand 2017; El-Taher 2010; Mohebian et al. 2019; Kashian et al. 2020). Natural radioactivity in building materials is due to the presence of ^{226}Ra, ^{232}Th decay chain products and ^{40}K element in them. It is essential to estimate the amount of exposure to radiation from building materials, as humans spend about 80% of their lives indoors. Therefore, using advanced methods can improve the accuracy of monitoring and evaluation of natural radiation levels (Mehdizade et al. 2011; Sivakumar et al. 2018; Lotfalinezhad et al. 2017; Ji et al. 2019).

So far, some studies have been done about this all over the world. In a study in Egypt, the radiation hazards from building materials using gamma spectroscopic analysis were investigated (El-Taher 2010). In another study in Malaysia, the natural radioactivity levels of rocks were evaluated (Alnour et al. 2014). There have also been a few studies in Iran. Mehdizade and et al. (2011) obtained the activity concentration of building materials collected from different parts of Iran. The radiological hazards due to the natural radioactivity of soil in Arak were also estimated (Pourimani and Davoodmaghami 2018). In most of these studies, the window (peak) analysis method was used. In this method, the activity of radionuclides is obtained only by taking into account the average activity of photo peaks of some daughter nuclides. Furthermore, the activity levels of radionuclides in the samples have been achieved by comparing methods using reference materials.

In this study, the activity concentration of ^{40}K, ^{232}Th and ^{226}Ra in different samples of building materials manufactured in Iran and used in Golestan province was measured by gamma ray spectrometry and using full spectrum analysis method. For this purpose, a relatively large NaI(Tl) scintillation detection system with high efficiency was used. The MCNPX Monte Carlo simulation

✉ Rahim Khabaz
r.khabaz@gu.ac.ir; ra_khabaz@yahoo.com

[1] Department of Physics, Faculty of Sciences, Golestan University, Gorgan 49138-15739, Iran

code was also used to determine the detector efficiency, the source self-absorption, and etc. Since the diversity levels of ^{40}K, ^{232}Th and ^{226}Ra distribution in the samples are not uniform, it will be convenient to use the radium equivalent activity (Ra_{eq}) to compare the specific activity of materials. Based on measurement results, radium equivalent activity, absorbed dose rate, annual effective dose rate, internal and external hazard indices associated with the different kinds of building materials were investigated.

2 Materials and Methods

2.1 Sample Preparation and Experimental Measurement

Twelve new samples of building materials including cement, brick, gypsum, lime, autoclaved aerated concrete (AAC) heat insulating cement block and white cement were collected from city stores in Golestan province. The weight of each sample was approximately 1 kg. The samples were crushed, powdered and screened with a 200-μm mesh to obtain the desired size. The samples were placed in a furnace at 105 °C for 8 h to eliminate humidity and then weighed attentively by a digital scale. After weighing, the samples were poured into 300-ml polystyrene plastic containers. In order to obtain a secular equilibrium within the samples, the containers were wholly sealed for one month. Secular equilibrium is a condition in which the rate of decay of the daughters and parent is equal. This step is necessary to ensure that radon gas confined within the volume and the decay products will also remain in the sample.

The detection system used in this study consisted of a NaI(Tl) scintillator detector (with a diameter of 10.16 cm and height of 10.16 cm) with relatively high efficiency, containing a photomultiplier tube (PMT) which was connected to a bias supply running at 900 V, a preamplifier, and a spectroscopy amplifier. The NaI(Tl) scintillator detector was surrounded by a 5-cm-thick cylindrical lead shield, while the whole detection system was placed in a lead box with a wall thickness of 5 cm to prevent background radiation from entering the detector. All pulses received from the amplifier and were digitalized by a multi-channel analyzer (MCA) and a computer. It should be noted that in order to set the MCA energy scale, the detection system was calibrated by ^{137}Cs and ^{60}Co sources. After calibration of the detection system, the sample container was placed directly on the detector. The counting time for each sample was set to 10,000 s, and 256 channels were selected for MCA. At the end of each counting, the live time of the detector was recorded, and the spectra were stored in the MCA. After counting of each sample, background radiation was measured to correct the peak area caused by the radionuclides in the samples as well as to obtain a net count of the radiation from the samples. Therefore, at each measurement for counting of background radiation, the empty sample container under the same conditions to the actual sample was placed on the detector. In order to obtain the net counts, the background radiation spectrum was subtracted from the energy spectrum of each sample.

2.2 Simulation of the Detection System

Detection of gamma rays emitted from building materials samples in a NaI(Tl) scintillation detector was modeled using MCNPX2.6 particle transport simulation code to obtain the response function and detector efficiency under irradiation of building materials samples. For this purpose, the container containing material like the real sample in measurement was simulated as a truncated cone with diameters of 10.1 cm and 8.8 cm and height of 4.5 cm at a distance of 0.5 cm from the detector. The gamma sources have randomly been assumed within the sample container volume, which emitted photons into 4π. Therefore, gamma conversion and self-absorption could be taken. Figure 1 shows the simulated detection system including, NaI(Tl) detector and sample container.

Three separate calculations were performed to estimate the energy spectrum of ^{40}K, ^{232}Th and ^{226}Ra radioisotopes. The gamma energy of the ^{40}K source was 1.4608 MeV. The gamma ray energies and probabilities for the ^{226}Ra and ^{232}Th decay series were considered based on Refs. (Evans 1983; Heath 1997). Finally, to obtain the detector response, an F8:p tally was used to create the pulse height spectrum (Khabaz and Yaghobi 2015). The pulse height tally provides the energy distribution of pulses created in a cell that models a physical detector. In MCNPX calculations, the

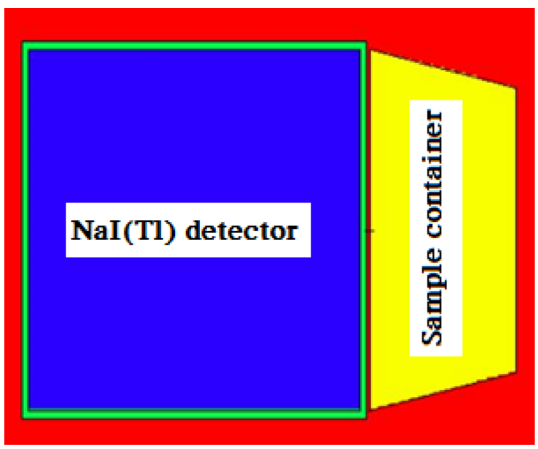

Fig. 1 The simulated detection system including NaI(Tl) detector and sample container

energy resolution of NaI(Tl) detector was defined as 10.73% at E_o = 0.662 MeV (i.e. the Gaussian energy broadening of MCNPX calculated pulse-height spectra was defined according to FWHM $= a + b\sqrt{E + cE^2}$, where a, b and c are user-supplied coefficients and E equals E_o). The parameters a, b and c previously were determined which are equal to -0.00419 MeV, 0.08591 $\text{MeV}^{1/2}$ and 0.20197 MeV^{-1}, respectively (Khabaz and Yaghobi 2014).

3 Result and Discussion

Figure 2 illustrates the measured net gamma energy spectrum of a typical sample using NaI(Tl) detector.

Figure 3 displays the simulated spectra of ^{40}K, ^{232}Th and ^{226}Ra for a typical sample achieved from three separated Monte Carlo programs. These spectra are normalized to one photon emitted by the source.

The measured pulse-height spectrum of each sample (dependent variable) can be related to three simulated spectra of ^{40}K, ^{232}Th and ^{226}Ra sources (independent variables) using multiple linear regression. This relationship is represented by the following linear equation in which C_{ex} is the dependent variable (experimental spectrum) and C_K, C_{Th} and C_{Ra} are independent variables (simulated spectrum)

$$C_{ex} = \beta_1 C_K + \beta_2 C_{Th} + \beta_3 C_{Ra}. \quad (1)$$

Multiple linear regression is done based on genetic algorithm (GA) applying R statistical computation software to estimate three scale factors ($\beta_{1,2,3}$) representing the distribution of ^{40}K, ^{232}Th and ^{226}Ra sources in the experimental spectrum.

For a multiple linear regression, it is customary to use the ordinary least squares method (OLS) to estimate the parameters of model. However, because of some limitations of this method some alternative approaches have been proposed to obtain more accurate model. The main obstacles for seriously misleading results of OLS method are existence dependence between observations, heterogeneity of observations, multi-collinearity between explanatory variables and outliers. Genetic algorithm is a class of evolutionary algorithm widely used for optimization. The algorithm includes three steps: (1) picking some possible values for parameters as starting values, (2) evaluating some criteria to express how the model works with a combination of parameters and (3) changing the values to establish the best solution. The genetic algorithm obtains robust solution with respect the mentioned limitation of OLS method and more precise parameter estimation. Following estimating the parameters, one can evaluate the quantities for describing and making further inferences about the model like coefficient of determination (χ^2), sum of squares, standard division of parameters and, etc.

A typical example of the full gamma spectrum fitting result is shown in Fig. 2, which the sum of the simulated spectra is shown as the solid line.

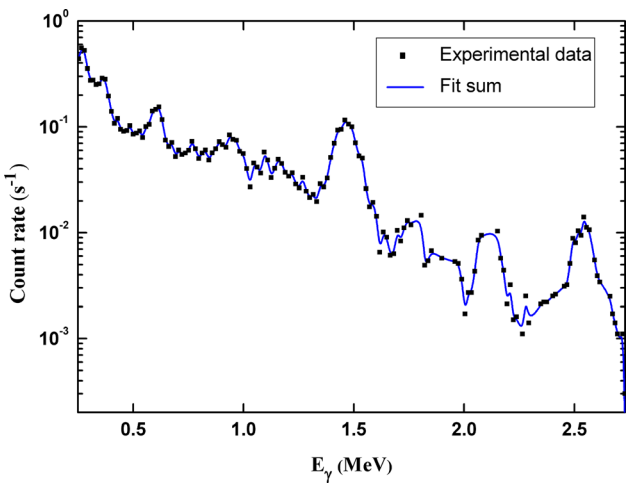

Fig. 2 The measured net energy spectrum of a typical sample with the full gamma spectrum fitting

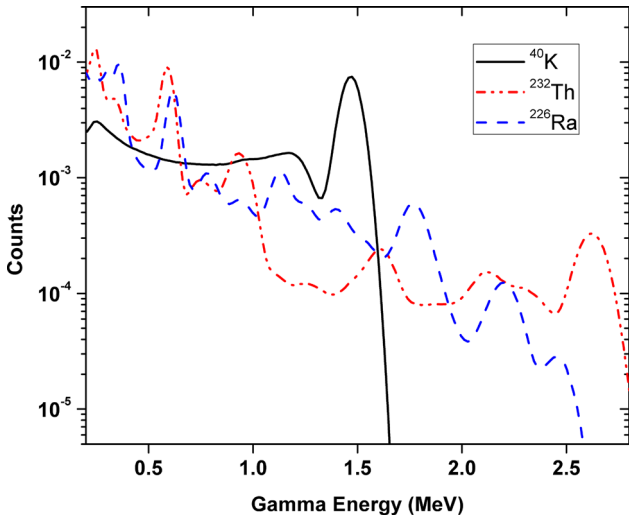

Fig. 3 The simulated spectra of ^{40}K, ^{232}Th and ^{226}Ra for a cement sample

3.1 Calculation of Activity Concentration

The radionuclide concentrations of ^{40}K, ^{232}Th and ^{226}Ra in different samples of the building materials were determined using gamma ray spectrometry method and by combining experimental measurement results and Monte Carlo calculations, including parameters such as detection efficiency, source self-absorption rate, etc.

The activity concentration of each radionuclide was assessed using the corresponding scale factor (β) which previously determined by linear regression (Eq. 1), and the

average number of gamma rays emitted per disintegration of the parent ($N_{\gamma/d}^{i}$) (Khabaz and Hassanvand 2017). The activity values were calculated by the following equation (Llope 2011):

$$A_i^j = \frac{\beta_i^j}{N_{\gamma/d}^{i} m_j} \quad (2)$$

where A_i^j is the specific activity in Bq kg^{-1}, j is the sample identification index, and m_j is the mass of each sample in kg. The activity concentrations of ^{40}K, ^{232}Th and ^{226}Ra obtained for different building materials are listed in Table 1.

The activity concentrations of ^{40}K, ^{232}Th and ^{226}Ra ranged from 36.79 to 559.82 Bq kg^{-1}, 1.29 to 36.01 Bq kg^{-1}, and 1.20 to 32.62 Bq kg^{-1}, respectively. The average values of 154.09 Bq kg^{-1}, 7.98 Bq kg^{-1} and 9.03 Bq kg^{-1} were also quantified for ^{40}K, ^{232}Th and ^{226}Ra, respectively.

It should be noted that Portland cement and gypsum are made with the standard mixture in all factories. However, the raw materials of each sample in different factories are prepared from different areas, which each of them can contain different amounts of radioactive material such as ^{40}K, ^{232}Th and ^{226}Ra. Sometimes these radioisotopes may be present as impurities in the sample formulation.

The mean values of [A_K, A_{Th}, A_{Ra}] previously measured for cement, gypsum, brick and cement block in Iran are [291, 28.9, 39.6 Bq kg^{-1}], [116, 2.2, 8.1 Bq kg^{-1}], [851, 12.2, 37 Bq kg^{-1}] and [436, 3.0, 20.7 Bq kg^{-1}], respectively (Mehdizade et al. 2011). A comparison between the mean values of radioactivity of materials (cement and brick) obtained in this study and the values in other countries are presented in Table 2 (Trevisi et al. 2012).

3.2 Radium Equivalent Activity (Ra_{eq})

The ^{40}K, ^{232}Th and ^{226}Ra radioisotopes are not uniformly distributed in building materials. Radium equivalent activity (Ra_{eq}) was applied to estimate the hazards related to materials containing ^{40}K, ^{232}Th and ^{226}Ra. This quantity was determined according to the assumption that 4810 Bq kg^{-1} of ^{40}K, 260 Bq kg^{-1} of ^{232}Th and 370 Bq kg^{-1} of ^{226}Ra represent the same gamma dose rate. This index was calculated using the following equation (UNSCEAR 2008):

$$Ra_{eq} = A_{Ra} + 1.43A_{Th} + 0.077A_K \quad (3)$$

where A_K, A_{Th} and A_{Ra} are the activity concentrations of ^{40}K, ^{232}Th and ^{226}Ra in Bq kg^{-1}, respectively, which presented in Table 1. The maximum amount of radium equivalent activity (Ra_{eq}) in building materials for safe use should not exceed 370 Bq kg^{-1} (UNSCEAR 2008). Table 3 shows the Ra_{eq} value for 12 samples of building materials ranged from 26.12 to 76.60 Bq kg^{-1} with the average value of 31.23 Bq kg^{-1} which is lower than the maximum value reported by UNSCEAR.

The average values of radium equivalent activity obtained for cement, gypsum, brick and cement block in Iran are 103.32, 20.19, 120.0 and 58.58 Bq kg^{-1}, respectively (Mehdizade et al. 2011). The mean radium equivalent activities calculated for cement, gypsum, brick and concrete block in some areas in the world are as follows: 82.5, 25, 128 and 61 Bq kg^{-1} in Egypt (Eissa et al. 2004), 79, 63, 180 and 94 Bq kg^{-1} in Zambia (Hayumbu et al. 1995), 115, 15, 833 and 85 Bq kg^{-1} in Australia, and 70, 41, 640 and 155 Bq kg^{-1} in Germany (Beretka and Mathew 1985).

Table 1 The measured activity concentration of ^{40}K, ^{232}Th and ^{226}Ra in building materials

No.	Sample	Density (g cm^{-3})	A_K (Bq kg^{-1})	A_{Th} (Bq kg^{-1})	A_{Ra} (Bq kg^{-1})
1	Shahrood Portland cement	3.25	52.29	5.79	12.07
2	Peyvand Portland cement	3.25	58.74	3.49	10.81
3	Joveyn Portland cement	3.25	61.10	1.47	6.93
4	Bojnord Portland cement	3.25	36.79	2.24	6.47
5	Semnan saleh gypsum	2.32	135.52	3.50	32.62
6	Semnan ayneh gypsum	2.32	559.82	19.34	8.01
7	Damghan brick	1.80	41.6	1.29	9.12
8	Gorgan brick	1.80	185.02	6.73	2.64
9	Ali abad fireproof brick	2.10	223.14	1.44	2.07
10	Sabzevar limestone	2.71	120.39	11.87	8.94
11	AAC cement block	2.25	252.08	36.01	7.46
12	Mashhad white cement	3.25	122.59	2.59	1.20
Average			154.09	7.98	9.03

Table 2 A comparison between radioactivity content of cement and brick in this study and other parts of the world (Trevisi et al. 2012)

Country	A_K (Bq kg^{-1})		A_{Th} (Bq kg^{-1})		A_{Ra} (Bq kg^{-1})	
	Cement	Brick	Cement	Brick	Cement	Brick
Iran (this study)	66.3	149.9	3.1	3.2	7.5	4.6
Austria	210	635	14	45	27	38
Belgium	255	692	46	37	52	41
Bulgaria	160	600	19	43	29	42
Cyprus	152	200	10	6	16	9
Czech	237	592	19	49	46	48
Denmark	90	455	12	21	20	25
Finland	251	804	20	42	40	52
France	24	–	21	53	35	51
Germany	170	453	73	46	86	50
Greece	257	680	19	35	85	53
Hungary	218	556	22	48	30	56
Ireland	131	482	11	31	60	42
Italy	357	672	63	30	41	37
The Netherlands	271	532	64	40	62	38
Poland	353	515	66	20	73	16
Portugal	256	786	19	52	31	64
Romania	233	501	27	47	44	45
Slovakia	223	695	18	44	35	49
Spain	305	569	40	68	61	54
Sweden	224	734	54	94	53	75

Table 3 The radium equivalent activity (Ra_{eq}), absorbed dose rate (D), annual effective dose rate (H_E) and external and internal hazard indices (H_{ex}, H_{in}) for building material samples

No.	Ra_{eq} (Bq kg^{-1})	D (nGyh^{-1})	H_E (μSvy^{-1})	H_{ex}	H_{in}
1	24.02	11.25	55.2	0.06	0.09
2	19.91	9.55	46.84	0.05	0.08
3	13.32	6.64	32.56	0.03	0.05
4	12.26	5.88	28.84	0.03	0.05
5	47.12	22.84	112.04	0.12	0.21
6	74.86	38.72	189.96	0.21	0.23
7	13.88	6.73	33	0.03	0.06
8	25.23	13.01	63.8	0.07	0.07
9	19.75	11.13	54.6	0.05	0.06
10	34.34	16.32	80.04	0.09	0.11
11	76.6	35.71	175.16	0.21	0.23
12	13.5	7.23	35.48	0.03	0.04
Average	31.23	15.42	75.64	0.08	0.11

3.3 Absorbed Dose Rate (*D*)

The activity concentration of ^{40}K, ^{232}Th and ^{226}Ra provides only information on the amount of those nuclei in the samples, while the absorbed dose rate is presented as an estimate of the effect of these radionuclides on the tissues of living creatures in the environment. According to the 2000 UNSCEAR report, the absorbed dose rate (D) is the energy absorbed in a matter per unit of time for a distance of 1 m top of a ground level calculated by the following equation (UNSCEAR 2000):

$$D\left[\text{nGyh}^{-1}\right] = 0.462A_{Ra} + 0.604A_{Th} + 0.0417A_K. \quad (4)$$

In this equation, A_K, A_{Th} and A_{Ra} are the activity concentrations of ^{40}K, ^{232}Th and ^{226}Ra, respectively, in the building materials samples. Table 3 presents the estimated absorbed dose rate for all building material samples. These values ranging from 5.88 to 38.72 nGyh^{-1} with the mean value of 15.42 nGyh^{-1}, which is lower than the permissible value (58 nGyh^{-1}) reported by UNSCEAR.

The mean values of absorbed dose rate determined for cement, gypsum, brick and cement block in Iran are 41.90, 8.80, 53.72 and 26.48 nGyh^{-1}, respectively (Mehdizade et al. 2011).

3.4 Annual Effective Dose Rate (AEDR)

The conversion coefficient and outdoor occupancy coefficient were used to determine the effective dose in each medium. A conversion factor (F = 0.7 Sv/Gy) was used for the conversion of the absorbed dose in the air to the

corresponding effective dose received by an adult. Also, 0.8 indoor occupancy fraction was taken into account, since the people spend 80% of their life inside buildings. The annual effective dose rate in μSvy^{-1} was calculated by the following equation:

$$H_E\left[\mu Svy^{-1}\right] = D \times T \times F \quad (5)$$

where D is the absorbed dose rate in terms of $nGyh^{-1}$, and T is irradiation time during the year, considering the outdoor occupancy coefficient ($0.8 \times 24\ h \times 365.25d$) and F conversion factor. The values of absorbed dose rate for each sample are listed in Table 3.

The mean values of annual effective dose rate acquired for cement, gypsum, brick and cement block in Iran are 290, 60, 370 and 180 μSvy^{-1}, respectively (Mehdizade et al. 2011).

3.5 Internal and External Hazard Indices (H_{ex}, H_{in})

At last, internal and external hazard indices were evaluated to ensure that the use of building materials is not harmful. These two indices must be less than unity. The external and internal hazard indices can be calculated through the following equations:

$$H_{ex} = \frac{A_{Ra}}{370} + \frac{A_{Th}}{259} + \frac{A_K}{4810} \quad (6)$$

$$H_{in} = \frac{A_{Ra}}{185} + \frac{A_{Th}}{259} + \frac{A_K}{4810}. \quad (7)$$

Table 3 indicates the results of H_{ex} and H_{in} for different samples, ranging from 0.03 (0.04) to 0.21 (0.23) with an average of 0.08 (0.11), which were less than unity. Therefore, the samples under investigation are safe to apply in the building.

The mean values of (H_{ex}, H_{in}) calculated for cement, gypsum, brick and cement block in Iran are (0.28, 0.39), (0.05, 0.08), (0.32, 0.42) and (0.16, 0.21), respectively (Mehdizade et al. 2011).

4 Conclusion

The activity concentrations of ^{40}K, ^{232}Th and ^{226}Ra in building materials used in Iran were measured by gamma ray spectrometry. The lowest ^{40}K, ^{232}Th and ^{226}Ra concentrations were found in samples No. 4, 7 and 12 and the highest in samples No. 6, 11 and 5, respectively. Also, the highest values for radium equivalent activity (Ra_{eq}), absorbed dose rate (D) and annual effective dose rate (H_E) were found in samples 11 and 6, respectively. From the results, it clear that the mean value of Ra_{eq} in the studied samples is lower than the internationally permissible value of 370 Bq kg^{-1}. The results showed that the values of internal and external hazard indices (H_{ex}, H_{in}), annual effective dose rate and absorbed dose rate were lower than those allowed by relevant international organizations. Hence, applying these building materials in construction are not a danger to the people.

Acknowledgements The authors are very grateful to Dr M. Azim-mohseni for his help and assistance in using the genetic algorithm by R statistical software.

References

Alnour IA, Wagiran H, Ibrahim N, Hamzah S, Elias MS, Laili Z, Omar M (2014) Assessment of natural radioactivity levels in rocks and their relationships with the geological structure of johor state, Malaysia. Radiat Prot Dosim 158:201–207

Arjomandi Z, Salehzadeh A, Mirzaie A (2018) Isolation and characterization of two novel radiation-resistant bacteria from a radioactive site in Iran. Iran J Sci Technol Trans Sci 42(3):1007–1013

Beretka J, Mathew PJ (1985) Natural radioactivity of Australian building materials, industrial wastes and by-products. Health Phys 48(1):87–95

Eissa EA, El-Khayat A, Ashmawy L, Hassan AM (2004) Studies on natural radioactivity of some Egyptian building materials. In: Proceedings of tlte environmental Pliysics conference, pp 121–129

El-Taher A (2010) Gamma spectroscopic analysis and associated radiation hazards of building materials used in Egypt. Radiat Prot Dosim 138:166–173

El-Taher A, Uosif MAM, Orabi AA (2007) Natural radioactivity levels and radiation hazard indices in granite from Aswan to Wadi El-Allaqi southeastern desert, Egypt. Radiat Protect Dosim 124(2):148–154

Evans ML (1983) Calculation of terrestrial gamma-ray fields in airborne radiometric surveys. Los Alamos National Laboratory, LS-9471-MS, N. Mex., USA

Hayumbu P, Zaman M, Lubaba N, Munsanje S, Muleya D (1995) Natural radioactivity in Zambian building materials collected from Lusaka. J Radioanal Nucl Chem 199(3):229–238

Heath RL (1997) Scintillation spectrometry gamma-ray spectrum catalogue, 2nd edn. Idaho National Laboratory, Idaho

Ji YY, Jang M, Lee W (2019) Development of the environmental radiation survey program and its application to in situ gamma-ray spectrometry. Health Phys 116(6):840–851

Kashian S, Saleh Kotahi M, Fathivand AA, Lotfalinezhad P (2020) Investigation of radiological hazards in soil of Mazandaran Province Iran. Iran J Med Phys. https://doi.org/10.22038/ijmp.2020.43527.1659

Khabaz R, Hassanvand M (2017) Radioactivity concentrations and dose characteristics of granite stones. Nucl Technol Radiat Prot 32:275–280

Khabaz R, Yaghobi F (2014) Evaluation of the nonlinear response function and efficiency of a scintillation detector using Monte Carlo and Analytical methods. Asian J Exp Sci 28(2):23–31

Khabaz R, Yaghobi F (2015) Design and employment of a non-intrusive *g*-ray densitometer for salt solutions. Radiat Phys Chem 108:18–23

Llope WJ (2011) Activity concentrations and dose rates from decorative granite countertops. J Environ Radioact 102:620–629

Lotfalinezhad P, Kashian S, Saleh Kotahi M, Fathivand A (2017) Estimation of natural radioactivity and radiation exposure in

environmental soil samples of Golestan, Iran. Iran J Med Phys 14(2):98–103

Mehdizade S, Faghihi R, Sina S (2011) Natural Radioactivity in building materials in Iran. Nukleonika 56:363–368

Mohebian M, Pourimani R, Modarresi SM (2019) Using MCNP simulation for self-absorption correction in HPGe spectrometry of soil samples. Iran J Sci Technol Trans Sci 43(6):3047–3052

Pangh B, Khabaz R, Izadpanah A (2019) Measurement of outdoor and indoor ambient gamma dose rate in Gorgan and Bandar-Torkman cities using gas and TLD dosimeters. Iran J Health Environ 12(3):397–408

Pourimani R, Davoodmaghami T (2018) Radiological hazard resulting from natural radioactivity of soil in East of Shazand power plant. Iran J Med Phys 15:192–199

Sivakumar S, Chandrasekaran A, Senthilkumar G, Gandhi MS, Ravisankar R (2018) Determination of radioactivity levels and associated hazards of coastal sediment from south east coast of Tamil Nadu with statistical approach. Iran J Sci Technol Trans Sci 42(2):601–614

Trevisi R, Risica S, D'alessandro M, Paradiso D, Nuccetelli C (2012) Natural radioactivity in building materials in the European Union: a database and an estimate of radiological significance. J Environ Radioact 105:11–20

UNSCEAR, United Nations Scientific Committee on the Effects of Atomic Radiation (2000) Sources, effects and risks of ionizing radiation and exposure from natural sources of radiation, United Nations, New York

UNSCEAR, United Nations Scientific Committee on the Effects of Atomic Radiation (2008) Sources, exposure from natural sources of radiation, United Nations, New York